Application of Phi29 Motor pRNA for Targeted Therapeutic Delivery of siRNA Silencing Metallothionein-IIA and Survivin in Ovarian Cancers

Pheruza Tarapore[1], Yi Shu[2], Peixuan Guo[2] and Shuk-Mei Ho[1]

[1]*Department of Environmental Health, College of Medicine, Center of Environmental Genetics, Cincinnati Cancer Center, University of Cincinnati, Cincinnati, Ohio, USA;* [2]*Nanobiomedical Center, College of Engineering & Applied Science/College of Medicine, University of Cincinnati, Cincinnati, Ohio, USA*

Ovarian cancer is a highly metastatic and lethal disease, making it imperative to find treatments that target late-stage malignant tumors. The packaging RNA (pRNA) of bacteriophage phi29 DNA-packaging motor has been reported to function as a highly versatile vehicle to carry small interference RNA (siRNA) for silencing of *survivin*. In this article, we explore the potential of pRNA as a vehicle to carry siRNA specifically targeted to metallothionein-IIa (*MT-IIA*) messenger RNA (mRNA), and compare it to *survivin* targeting pRNA. These two anti-apoptotic cell survival factors promote tumor cell viability, and are over-expressed in recurrent tumors. We find that pRNA chimeras targeting *MT-IIA* are processed into double-stranded siRNA by dicer, are localized within the GW/P-bodies, and are more potent than siRNA alone in silencing *MT-IIA* expression. Moreover, knockdown of both *survivin* and *MT-IIA* expression simultaneously results in more potent effects on cell proliferation in the aggressive ovarian tumor cell lines than either alone, suggesting that therapeutic approaches that target multiple genes are essential for molecular therapy. The folate receptor–targeted delivery of siRNA by the folate-pRNA dimer emphasizes the cancer cell–specific aspect of this system. The pRNA system, which has the capability to assemble into multivalent nanoparticles, has immense promise as a highly potent therapeutic agent.

Received 8 January 2010; accepted 14 October 2010; published online 9 November 2010. doi:10.1038/mt.2010.243

INTRODUCTION

Ovarian cancer is a highly metastatic and lethal disease with an estimated 13,850 deaths annually and 21,880 new cases diagnosed in 2010. It has the highest mortality of all cancers of the female reproductive system, although it is treatable when detected early. Unfortunately, most diagnoses occur at advanced stages of disease, when the cancer has usually metastasized, spread beyond the ovary, and is difficult to treat.

Survivin has a pivotal role in tumor cell survival (reviewed in Altieri[1]) and is differentially expressed in ovarian tumor cells as compared to most normal tissues.[2–4] *Survivin* expression correlates with proliferative index, clinical stage, histological grade, clinical outcome, and survival rate in epithelial ovarian and endometrial carcinomas.[2–4] Preclinical studies have demonstrated that downregulation of *survivin* expression or function reduced tumor growth potential and increased tumor cell apoptotic rate in various human tumor models (reviewed in Pennati *et al.*[5]). These factors make *survivin* an attractive target for gene therapy.

Metallothionein (MT) family of metal-binding proteins confers protection against apoptosis[6] and plays an important role in cell proliferation;[7] both processes are important in carcinogenesis. The increased expression of MT in malignant as opposed to benign ovarian surface epithelial tumors and also with increasing histological grade tumors[8,9] suggests a role for MT in tumorigenesis. To date, there are seven MT-I functional isoforms, but only one MT-II functional isoform (named MT-IIA) characterized. The survival of mice lacking functional *MT-I* and *MT-IIA* genes[10] indicates that these proteins are not crucial factors for normal cell survival.[10] However, silencing *MT-IIA* expression induces apoptosis in cancer cells,[11–13] without augmenting the expression of *MT-I* isoforms, making *MT-IIA* a candidate for therapeutic intervention.

There has been an increased interest in RNA interference (RNAi) as a therapeutic approach for treatment of cancer. There is accumulating evidence that delivery of small interference RNA (siRNA) (targeting anti-apoptotic genes) as dicer-substrate siRNA (d-siRNA—27 bp) can be up to a 100-fold more potent than the traditional 21-mer siRNA.[14–16] Moreover, by coupling synthetic d-siRNA with a cancer cell–specific ligand or a RNA aptamer[17,18] targeted toward a cancer-specific receptor, one can potentially target delivery of d-siRNA only to cancer cells. This mode of d-siRNA delivery is gaining importance because the preformed d-siRNA is extremely potent at gene silencing, is short lived,[19,20] and is rapidly cleared by the system, eliminating long-term effects. Another approach to deliver siRNA into cells for gene therapy is with packaging RNA (pRNA) of bacteriophage phi29.[21–24]

Correspondence: *Shuk-Mei Ho, Department of Environmental Health, Kettering Complex, Room 128, 3223 Eden Avenue, University of Cincinnati, P.O. Box 670056, Cincinnati, Ohio 45267, USA. E-mail: Shuk-mei.Ho@uc.edu*

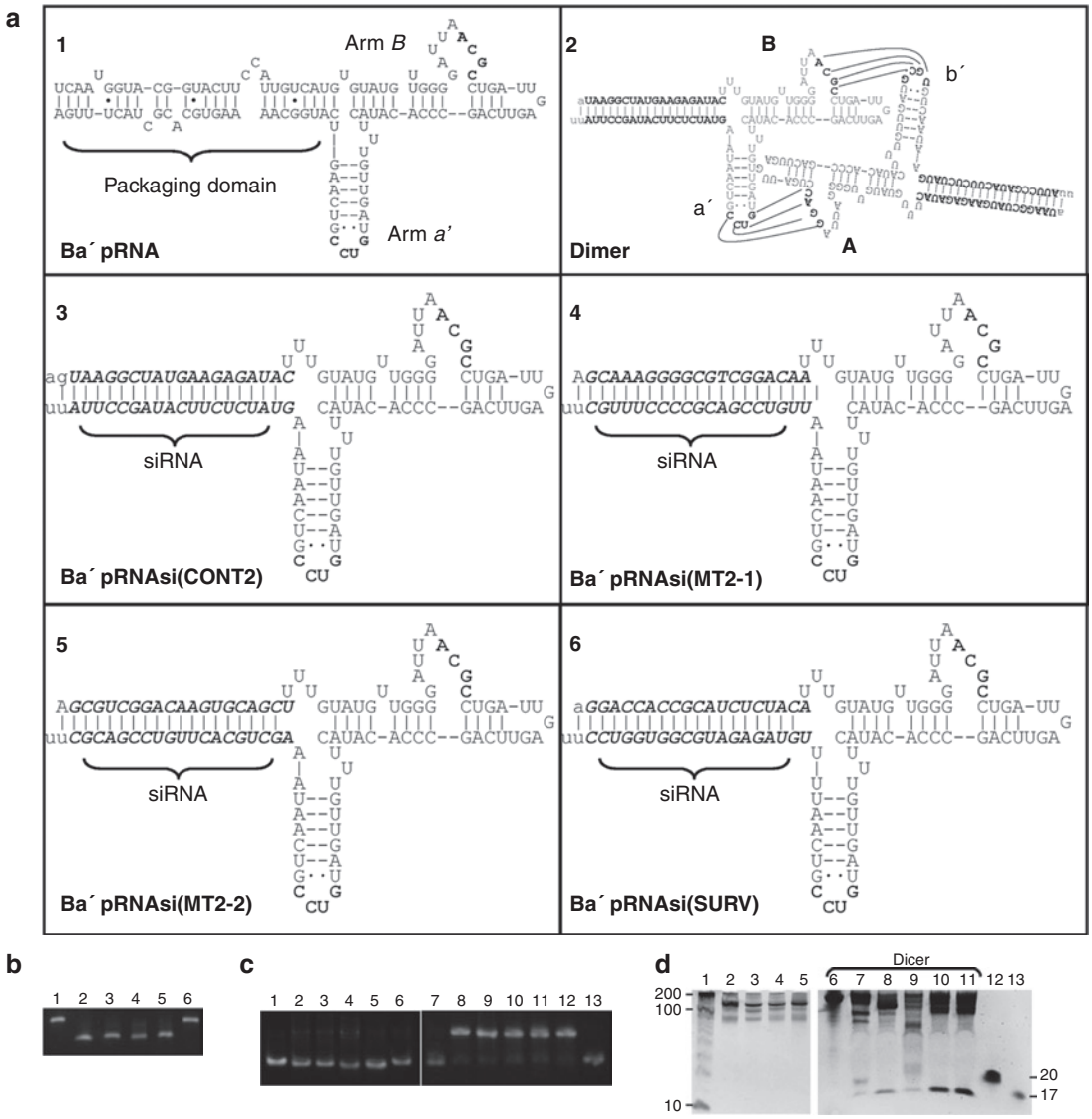

Figure 1 Sequence and structure of pRNA chimera. (**a**) Sketch of chimeric siRNA harbored in pRNA vector. (**a**) Sequence and secondary structure of (1) Ba'pRNA, (2) Ab'pRNA/si(CONT2) and Ba'pRNA/si(CONT2) dimer, (3) Ba'pRNA/si(CONT2) (control siRNA), (4) Ba'pRNA/si(MT2-1), (5) Ba'pRNA/si(MT2-2), and (6) Ba'pRNA/si(Surv). All chimeras have identical pRNA backbone sequence, whereas the sequence of siRNA are altered. (**b**) The pRNA/siRNA have the correct size. The Ab'pRNA, Ba'pRNA/si(MT2-1), Ba'pRNA/si(MT2-2), Ba'pRNA/si(Surv) and Ba'pRNA/si(CONT2) and Ba'pRNA (lanes 1–6) were transcribed and analyzed on a 6% denaturing gel. (**c**) The pRNA/siRNA have the correct intermolecular interactions. The Ba'pRNA, Ba'pRNA/si(MT2-1), Ba'pRNA/si(MT2-2), Ba'pRNA/si(Surv), and Ba'pRNA/si(CONT2) (lanes 1–5, 8–12) were analyzed on a 6% nondenaturing gel in the absence (monomers, lanes 1–5) and presence (dimers, lanes 8–12) of Ab'pRNA. The migration of the monomer Ab'pRNA (lanes 6, 7) and Ba'pRNA (lane 13) is also shown. (**d**) Processing of chimeric pRNA/siRNA complex into siRNA by purified dicer. The Ba'pRNA, Ba'pRNA/si(MT2-1), Ba'pRNA/si(MT2-2), Ba'pRNA/si(Surv), and Ba'pRNA/si(CONT2) (lanes 1–5, 6–10) were incubated in the absence (lanes 1–5) or presence (lanes 6–10) of dicer for 1 hour, and analyzed by 8% denaturing gel. Lane 11 represents Ba'pRNA/si(CONT2) incubated with dicer for 3 hours.

pRNA is a component of the bacteriophage phi29 DNA-packaging motor.[25,26] pRNA (**Figure 1a**) can form dimers, trimers, and hexamers.[24,27,28] Each pRNA contains two functional domains. The central domain of pRNA contains two interlocking left hand and right hand loops that can be engineered to form stable intermolecular loop–loop interactions[27] (**Figure 1a**). The DNA-packaging domain is located at the 5′/3′ paired ends.[29] The two domains fold separately, and replacement of the packaging domain with siRNA does not affect pRNA structure, folding, or intermolecular interactions.[29,30] The resultant pRNA/siRNA chimera is useful for gene therapy.

We have previously shown that the pRNA/si(Surv) chimera can be used for the delivery of siRNA targeting *survivin* into breast, prostate, and nasopharyngeal carcinoma cells.[21–23] In this report, we explore the potential use of pRNA to carry siRNA specific for *MT-IIA*, and compare its efficacy to induce cell death with that of a *survivin* targeting pRNA in ovarian cancer cells. We show that the pRNA/siRNA can be processed by dicer, and can downregulate *MT-IIA* and *survivin* messenger RNA (mRNA) levels when introduced into cells, resulting in decreased cell proliferation. Moreover, the pRNA/si(MT2A) is more efficient than the synthetic 21-mer siRNA alone, in silencing *MT-IIA* expression. Finally, we show that

Ba′pRNA/si(MT2A) can form dimers with folate-tagged pRNA (folate-pRNA), bind to cells expressing folate receptor, and inhibit cell growth. Thus, the folate-pRNA can be used to deliver pRNA targeting expression of *MT-IIA* or *survivin* to ovarian cancer cells, making it a highly potent therapeutic agent.

RESULTS

Construction of pRNA/siRNA chimera

Phi29 pRNA contains a DNA-packaging domain as well as an intermolecular interacting domain with complementary left and right hand loops/arms (**Figure 1a**). To construct the pRNA/siRNA chimeras targeting either *MT-IIA* or *survivin*, the 5′/3′ helical DNA-packaging domain was replaced by the respective siRNA (**Figure 1a**), or by a random sequence as a control. The transcribed RNA was analyzed on a denaturing gel to verify the correct size of the pRNA/siRNA chimera (**Figure 1b**). As expected, the 110 nt Ba′pRNA/si(MT2-1), Ba′pRNA/si(MT2-2), Ba′pRNA/si(Surv), and Ba′pRNA/si(CONT2) (**Figure 1b**, lanes 2–5) ran slightly faster than the 117 nt Ab′pRNA and Ba′pRNA (**Figure 1b**, lanes 1, 6). To confirm that the Ba′pRNA/siRNA chimeric complexes retained their correct folding and capability for intermolecular interaction, Ba′pRNA/siRNA chimeras were mixed with Ab′pRNA and analyzed on a nondenaturing gel. The Ba′pRNA and Ba′pRNA/siRNA chimeras did not homodimerize (see Materials and Methods, **Figure 1c**, lanes 1–5, monomers) and efficiently formed heterodimers with Ab′pRNA (**Figure 1c**, lanes 8–12) as indicated by change in mobility of the bands.

The pRNA/siRNA construct is processed by dicer

Next, to confirm that the Ba′pRNA/siRNA chimeras could be processed into siRNA by dicer *in vitro*, chimeric pRNA/siRNA were treated with purified recombinant dicer, which processes long double-stranded RNA into siRNAs. We had previously shown by 5′ end ^{32}P end-labeling that a 22-base siRNA can be generated with high efficiency by pRNA/siRNA chimera digestion with dicer.[21] Purified Ba′pRNA/siRNA chimeras were mixed with dicer, and the digested product was then analyzed on denaturing polyacrylamide gel electrophoresis (PAGE)/urea gels. As shown in **Figure 1d**, digestion of the pRNA/siRNA chimeras by dicer resulted in production of 17–22-base siRNA (**Figure 1d**), which are absent in the nondicer containing lanes. This result confirms that similar to d-siRNA, the chimeric pRNA/siRNA is cleaved by dicer, and the double-stranded siRNA located at the 5′/3′ ends, are released.

Specific silencing of *MT-IIA* and *survivin* mRNA by their respective pRNA/siRNA chimera

Quantitative real-time-reverse transcription–PCR (qRT-PCR) was performed to evaluate the *MT-IIA* and *survivin* gene expression in the highly metastatic SKOV-3 cell line, as well as two primary ovarian cancer cell lines OVCA 432 and OVCA 433 obtained from patients with late-stage serous ovarian adenocarcinoma.[31,32] The mRNA from all three cell lines was analyzed by qRT-PCR for *MT-IIA* and *survivin* expression. The expression of *MT-IIA* mRNA was found to be high in all three cell lines with SKOV-3 cells showing highest expression (**Figure 2a**), with comparative threshold (C_t) values of 18 per 3 ng mRNA, corresponding to around

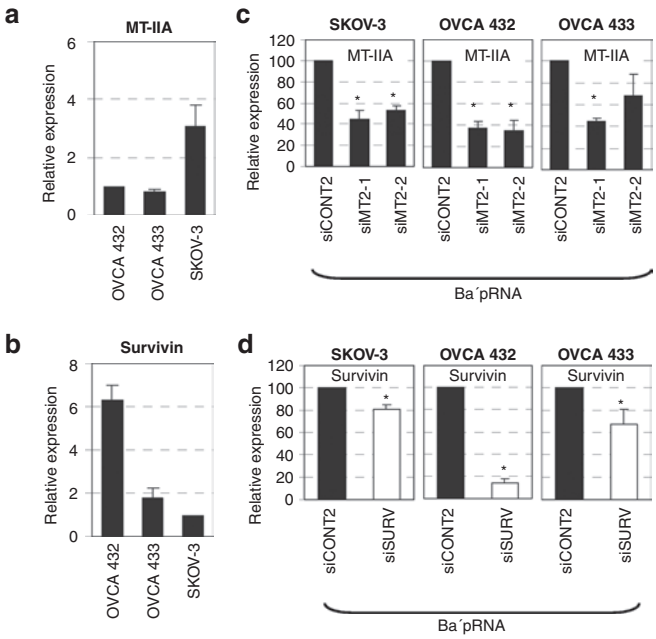

Figure 2 Ovarian cell lines express high levels of *MT-IIA* and *survivin* mRNA, and their silencing. Total RNA was extracted from OVCA 432, OVCA433, and SKOV-3 ovarian cell lines transfected with the pRNA/siRNA indicated after 24 hours, was reverse transcribed to cDNA, and was analyzed for mRNA expression by qRT-PCR. Values were normalized to GAPDH levels in the respective cell line. Error bars represent the SEM of three experiments, each performed in triplicate. Asterisk indicates statistically significant ($P < 0.05$). (**a**) Expression levels of *MT-IIA* are shown relative to those expressed in OVCA 432. (**b**) Expression of *survivin* mRNA are shown relative to those expressed in SKOV-3 cells. (**c**,**d**) Silencing the *MT-IIA* and *survivin* gene with Ba′pRNA/siRNA downregulate target gene expression at mRNA level. The graph represents the relative expression of *MT-IIA* (**c**) and *survivin* (**d**) in Ba′pRNA/si(CONT2), Ba′pRNA/si(MT2-1), Ba′pRNA/si(MT2-2), and Ba′pRNA/si(Surv) (2 nmol/l each) transfected SKOV-3, OVCA 432, and OVCA 433 cells as indicated. The expression levels are shown relative to control Ba′pRNA/si(CONT2)-transfected cells.

400,000 copies of *MT-IIA*. The *survivin* C_t values were also high, with OVCA 432 cells showing highest expression (**Figure 2b**). Next, we transfected the pRNA/siRNA into cells and examined these cells for suppression of *MT-IIA* and *survivin* mRNA expression. *MT-IIA* (**Figure 2c**) and *survivin* (**Figure 2d**) mRNA was decreased within 24 hours after transfection with Ba′pRNA/si(MT2-1), Ba′pRNA/si(MT2-2), and Ba′pRNA/si(Surv), as compared with the control [Ba′pRNA/si(CONT2)]. This indicates that pRNA/siRNA can specifically silence expression of their respective target mRNAs.

Decreased proliferation of ovarian cancer cells transfected with the chimeric pRNA/siRNA

Previous studies have shown that downregulation of *MT-IIA*[11–13,33] or *survivin* (recently reviewed[5]) can result in cell death due to apoptosis. To examine whether chimeric Ba′pRNA/siRNA targeting *MT-IIA* and *survivin* can decrease cell survival, we performed cell proliferation assays 3 days post-transfection. Cells transfected with Ba′pRNA/si(MT2-1), Ba′pRNA/si(MT2-2), and Ba′pRNA/si(Surv) exhibited decreased cell proliferation compared with cells transfected with control Ba′pRNA/si(CONT2) (**Figure 3a**).

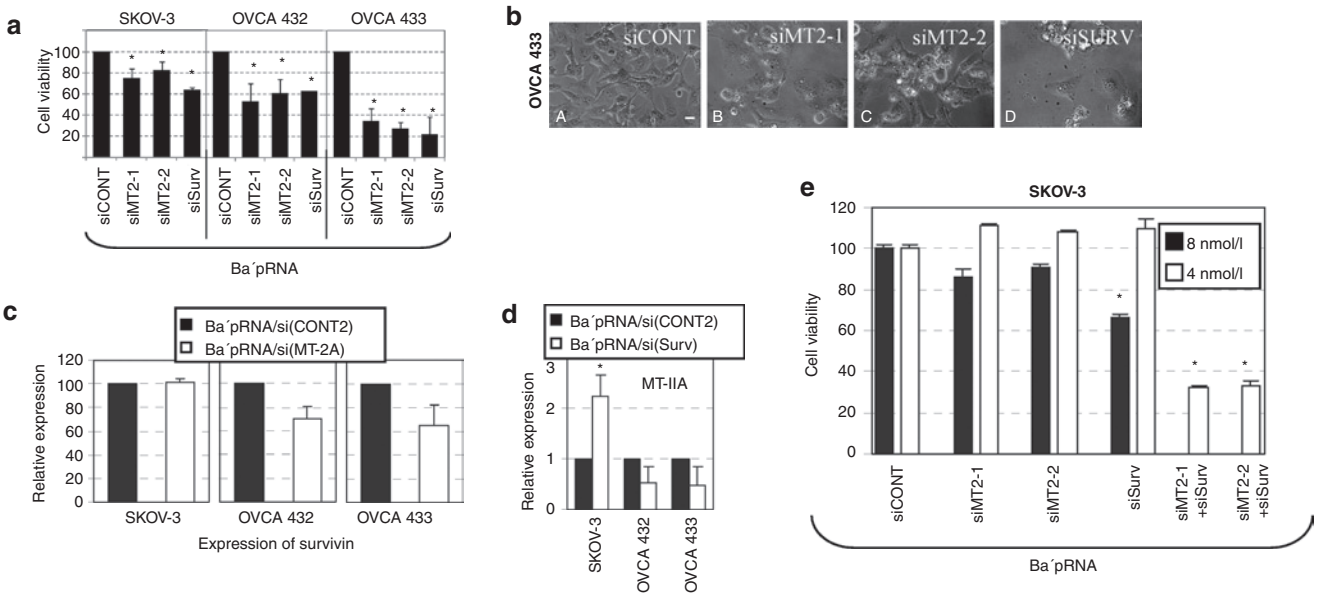

Figure 3 Silencing of *MT-IIA* or *survivin* expression inhibits cell proliferation in ovarian cancer cells. Results are presented as average ± SEM of triplicate experiments. Asterisk indicates *t*-test $P < 0.05$ when compared to respective control cells. (**a**) Cell proliferation assays at 72 hours post-pRNA/siRNA transfections (8 nmol/l each) as indicated. (**b**) Cell morphology of OVCA 433 cells after transfection with chimeric pRNA/siRNA. OVCA 433 cells were transfected with pRNA/siRNA chimeras as indicated and images were taken using an inverse microscope 72 hours post-transfection. Scale bar ~10 µmol/l. (**c**,**d**) *Survivin* and *MT-IIA* mRNA expression in Ba′pRNA/siRNA- (2 nmol/l each) transfected cells. Cells were transfected with Ba′pRNA/siRNA chimeras as indicated and the levels of *survivin* (**c**) and *MT-IIA* (**d**) mRNA determined at 24 hours. Results are presented relative to Ba′pRNA/si(CONT2)-transfected cells, after normalization to GAPDH values. (**e**) Silencing of *MT-IIA* and *survivin* expression results in enhanced decrease in cell survival in SKOV-3 cells. Cell proliferation assays at 72 hours post-pRNA/siRNA transfection at concentrations indicated.

Moreover, when examined under a microscope, the majority of Ba′pRNA/si(MT2A)- and Ba′pRNA/si(Surv)-transfected cells were rounded with dark condensed nuclei, and detached from the cell culture plate (**Figure 3b**). However, we noticed that the highly metastatic SKOV-3 cells consistently showed higher levels of cell survival compared to OVCA 432 and OVCA 433 cells (**Figure 3a**), when transfected with Ba′pRNA/si(MT2A). We examined the transfection efficiency by co-transfecting each pRNA/siRNAs along with pGFP, and counting the number of GFP-positive cells, and by transfecting Cy3-labeled pRNA/si(CONT2), into the three cell lines. We found that there was no significant difference among the cell lines, and their transfection efficiencies were comparable (70–90% for pRNA/siRNA). Because expression of both *MT-IIA* and *survivin* give cells a survival advantage, we examined the levels of *survivin* mRNA within the Ba′pRNA/si(MT2-1)- and Ba′pRNA/si(MT2-2)-transfected cells. Whereas transfection of Ba′pRNA/si(MT2A) led to decrease in *survivin* expression in OVCA 432 and OVCA 433 cells, such a decrease was not observed in SKOV-3 cells (**Figure 3c**). Moreover, when we examined *MT-IIA* expression in Ba′pRNA/si(Surv)-transfected SKOV-3 cells, an increase in *MT-IIA* expression (**Figure 3d**) was found, implying a compensatory effect of *survivin* silencing on *MT-IIA* expression. Transfection of any of the three Ba′pRNA/siRNAs had no effect on the expression levels of *Bcl-2* mRNA, another anti-apoptotic gene examined, indicating that this phenomenon was not a nonspecific effect (results not shown). Finally, SKOV-3 cells were co-transfected with either Ba′pRNA/si(MT2-1) or Ba′pRNA/si(MT2-2), and Ba′pRNA/si(Surv), to determine whether the combination would be more potent than either alone. Indeed, SKOV-3 cells silenced for *MT-IIA* and *survivin* showed a ~70% decrease in cell survival (**Figure 3e**).

It has been shown that T7 RNA polymerase–transcribed siRNA with the 5′ end phosphate group intact (pppG) can elicit interferon (IFN)-α and IFN-β expression leading to nonspecific inhibitory effects on cells.[34] Hence, we examined OVCA 433 cells transfected with the Ba′pRNA/siRNA for IFN-α and IFN-β expression, and found it to be negligible (**Supplementary Figure S1**).

The inhibitory function of the pRNA/siRNA is more potent than the 21-base synthetic double-stranded siRNA

Recent observations regarding the more potent interfering function of d-siRNA[18] indicate that the chimera pRNA/siRNA should also be more effective than the 21-base siRNA in its inhibitory function. To compare the relative potencies of 21-mer siRNA and pRNA/siRNA, we transfected OVCA 433 cells with both Ba′pRNA/siRNA and the 21-mer siRNA targeted to *MT-IIA*. Compared to pRNA/siRNA-transfected cells, we found that higher molar amounts of siRNA were required to obtain equivalent *MT-IIA* gene silencing. That is, although 2 nmol/l of Ba′pRNA/si(MT2-1) and Ba′pRNA/si(MT2-2) were sufficient to induce 40–50% decrease in *MT-IIA* levels (**Figure 2c**), 33 nmol/l of the 21-mer siRNA was required to knockdown the equivalent amount (**Figure 4a**). This effect was reflected in the cell proliferation. Whereas a significant decrease in cell proliferation was obtained with 2 and 8 nmol/l of Ba′pRNA/si(MT2-1) and Ba′pRNA/si(MT2-2) (**Figure 4b**), equivalent amounts of siMT2-1 and siMT2-2 did not have any effect on cell survival. A maximum of 20% decrease in cell

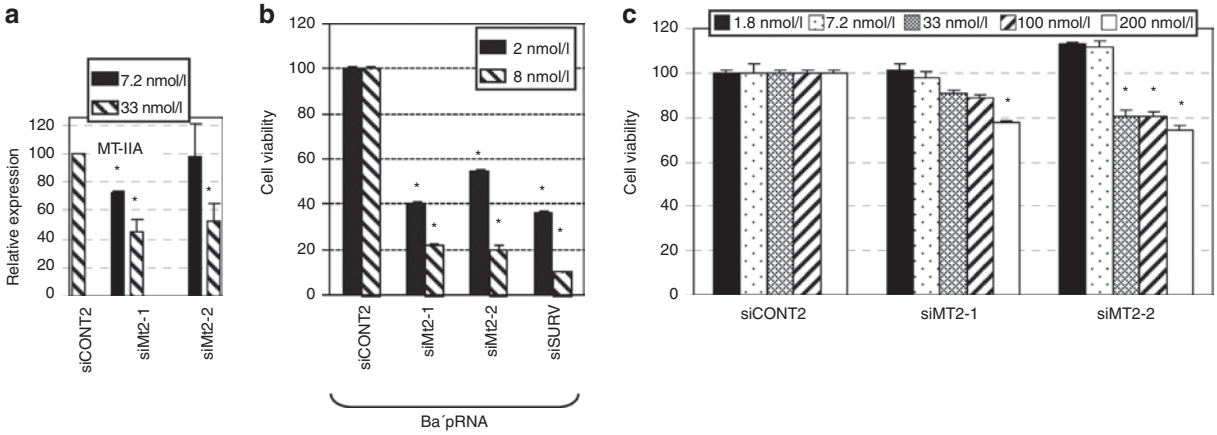

Figure 4 The RNAi function of pRNA/siRNA is more potent than siRNA. *MT-IIA* or *survivin* expression inhibits cell proliferation in OVCA 433 cells. Results are presented as average ± SEM of triplicate experiments. Asterisk indicates *t*-test $P < 0.05$. (**a**) *MT-IIA* mRNA expression is downregulated in siRNA-transfected cells. Cells were transfected with siCONT2, siMT2-1, and siMT2-2 as indicated, and the levels of *MT-IIA* mRNA determined at 24 hours post-transfection. Results are presented relative to siCONT2-transfected cells, after normalization to GAPDH values. (**b**) Cell proliferation assays at 72 hours post-pRNA/siRNA transfections at concentrations indicated. Average of two experiments. (**c**) Cell proliferation assays at 72 hours post-21-mer siRNA transfections at concentrations indicated.

proliferation was obtained with 33–200 nmol/l siRNA, indicating that the interfering effect is not as potent in 21-mer siRNA-transfected cells (**Figure 4c**). Similar effects on cell viability have been reported by other researchers[13] with the 21-mer siRNA in breast cancer cells. This provides evidence that our pRNA chimera system is more efficient than a 21-mer siRNA-based system, with greater therapeutic value.

The pRNA/siRNA chimera are present within the GW/P bodies

The mammalian GW182 protein, a major component of P-bodies,[35] has been found to colocalize and coimmunoprecipitate with Argonaute (Ago) proteins.[35,36] It has been shown that the GW182 protein interaction with Ago2 and their colocalization at multivesicular bodies are important in microRNA- and siRNA-mediated RNAi.[37,38] Although the exact role of GW182 is not known, it has been proposed that RISC (RNA-induced silencing complex) plays a role in targeting mRNAs to GW-rich bodies[38] where the mRNA is either degraded or translationally repressed. We thus determined whether the pRNA/siRNA chimeras localize within the GW/P-body complex. The pRNA/si(CONT2) chimera was labeled with Cy3 (**Figure 5a**) so that it could be tracked to investigate its subcellular localization in OVCA 433 cells. As a control, the FITC-siRNA (Invitrogen, Carlsbad, CA) was employed. Live image microscopy was performed. The Cy3 signal of pRNA/si(CONT2) was localized within discrete speckles within the cytoplasm (**Figure 5b**, 1–3), compared to a predominant nuclear and a uniform cytoplasmic appearance of the FITC-siRNA signal (**Figure 5b**, 4–6). However, it should be noted that some speckles were also observed in the FITC-siRNA-transfected cells (**Supplementary Figure S2**). Moreover, the Cy3 signal persisted for 6 days post-transfection, compared to the siRNA signal which faded within 72 hours (**Supplementary Figure S2**). The signal pattern obtained with Cy3-pRNA/si(CONT2) was similar to that obtained with siRNA- and miRNA-processing proteins Ago2 and GW182.[35,39,40] Therefore, we immunostained OVCA433

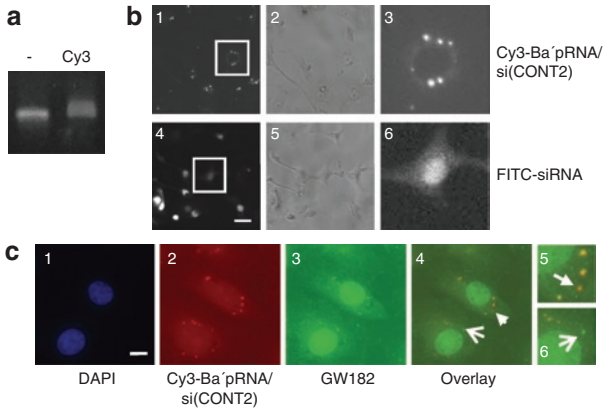

Figure 5 Ba´pRNA/si(CONT2) is localized to GW/P-bodies. (**a**) The Ba´pRNA/si(CONT2) was labeled using the Cy3 Silencer siRNA labeling kit (Ambion, Austin, TX). The resultant Cy3-pRNA/si(CONT2) was analyzed on a 8% denaturing gel. (**b**) OVCA 433 cells were transfected with Cy3-pRNA/si(CONT2) (1–3) and FITC-siRNA (4–6). Cells were examined after 24 hours using an inverted fluorescent microscope. Scale bar represents 20 µmol/l. Panels 3, 6 represent enlargements of the boxed areas (**c**) The Cy3-pRNA/si(CONT2)- (1–6) transfected cells were fixed and immunostained with mouse anti-GW182 antibody, followed by Alexa Fluor 488 chicken anti-mouse secondary antibody. Arrows point to non-overlapping signals. The closed and open arrows in panel 4 is further magnified in panels 5 and 6. Scale bar represents 5 µmol/l.

cells expressing Cy3-pRNA/si(CONT2) with mouse anti-GW182 antibody to determine whether the Cy3 signal was localized within the GW-bodies. We found that some of the Cy3-pRNA/si(CONT2) signal colocalized with the GW182 positive signal (**Figure 5c**), indicating that the pRNA/siRNA are present at sites involved in mRNA degradation.

Targeted delivery of folate-tagged pRNA into ovarian cancer cells

The ability of pRNA nanoparticle[30] to form dimers makes it extremely useful for targeted delivery of siRNA into cancer cells.

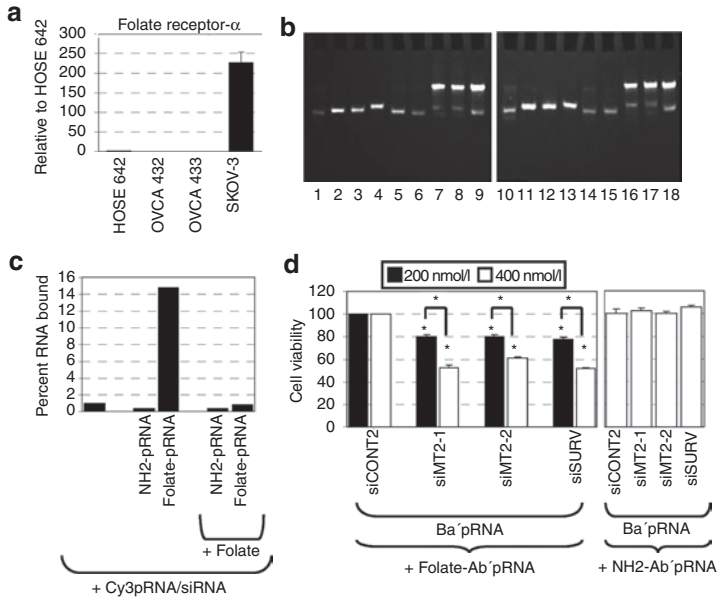

Figure 6 Targeted delivery of folate-tagged pRNA into ovarian cancer cells. (**a**) SKOV-3 cells express high levels of folate receptor-α mRNA. Total RNA was extracted from HOSE 642, OVCA 432, OVCA433, and SKOV-3 cell lines, was reverse transcribed to cDNA, and was analyzed for mRNA expression by qRT-PCR. Values were normalized to GAPDH levels in the respective cell line. Error bars represent the SEM of three samples each, each performed in triplicate. Expression levels of *survivin* are shown relative to HOSE 642 cells. (**b**) The Ba′pRNA/siRNA can dimerize with folate-Ab′pRNA. The Ba′pRNA/siRNA was incubated with folate-Ab′pRNA and analyzed on a nondenaturing gel. The 22/98 *Sph*I Ab′pRNA (lanes 1, 10), Ab′pRNA (lanes 2, 11), Ba′pRNA (lanes 3, 9, 12, 18), folate-Ab′pRNA (lanes 4, 13), Ba′pRNA/si(MT2-1) (lanes 5, 7), Ba′pRNA/si(MT2-2) (lanes 6, 8), Ba′pRNA/si(Surv) (lanes 14, 16), and Ba′pRNA/si(CONT2) (lanes 15, 17) were analyzed on a 6% nondenaturing gel in the absence (monomers, lanes 1–6, 10–15) and presence (dimers, lanes 7–9, 16–18) of folate-Ab′pRNA. (**c**) The folate-pRNA-Cy3-pRNA/siRNA binds to KB cells. Cells maintained in folate-free media were treated with the indicated Cy3-pRNA/siRNA dimer with either folate-pRNA or NH_2-pRNA. Flow cytometric analysis was performed to determine the percent of cells bound by Cy3-pRNA/siRNA. (**d**) Effects of targeted silencing *MT-IIA* or *survivin* expression in SKOV-3 cells. SKOV-3 cells were treated with the dimers formed above. Cell proliferation assays were performed 72 hours post-pRNA/siRNA treatment as indicated.

That is, the Ba′pRNA/siRNA form dimers with folate-Ab′pRNA for delivery into folate receptor expressing ovarian cancer cells. A number of researchers have found that folate receptor-α is highly expressed in ovarian carcinomas compared to normal tissue, with nearly 89% ovarian carcinomas staining positive for folate receptor.[41] We examined ovarian cancer cell lines for folate receptor-α expression by qRT-PCR and found highest levels in SKOV-3 cells (**Figure 6a**). Next, we made the folate-Ab′pRNA (as outlined in Materials and Methods) and confirmed that the folate moiety does not interfere with the heterodimerization of Ab′pRNA with Ba′pRNA/siRNA chimeras. The Ba′pRNA/siRNA chimeras were mixed with folate-Ab′pRNA and analyzed on a nondenaturing gel. The change in mobility of the bands indicates that the folate-pRNA (**Figure 6b**, lane 4, 7, 8, 13, 16, 17) can efficiently form dimers with Ba′pRNA/siRNA chimeras (**Figure 6b**, lanes 7, 8, 16, and 17). The positive control, Ab′pRNA-Ba′pRNA (**Figure 6b**, lanes 9, 18) runs as a dimer and the individual pRNA/siRNA run as monomers (lanes 1–3, 5, 6, 10–12, 14, 15). We determined the ability of folate-pRNA-Cy3-pRNA dimer to bind cells which express folate receptor-α by flow cytometry (**Figure 6c**) and confocal image microscopy (**Supplementary Figure S5**) as described in Materials and Methods. As shown in **Figure 6c**, we found that ~15% of cells are bound by folate-pRNA-Cy3-pRNA dimer, whereas <1% of cells are bound by Cy3-pRNA, or NH_2-pRNA-Cy3-pRNA dimer (negative controls). Moreover, we could compete the binding of folate-pRNA-Cy3-pRNA dimer to cells with free folate (**Figure 6c**). Finally, we treated SKOV-3 cells with folate-pRNA-pRNA/siRNA dimers. We obtained a statistically significant decrease in expression of *MT-IIA* and *survivin* on treatment with the respective RNA (**Supplementary Figure S6**). Moreover, we found a statistically significant 20–45% decrease in cell survival on treatment with folate-pRNA-Ba′pRNA/si(MT2-1), folate-pRNA-Ba′pRNA/si(MT2-2), and folate-pRNA-Ba′pRNA/si(Surv) (**Figure 6d**) compared to control-treated cells. Treatment with control pRNA-Ba′-pRNA/siRNA dimers without folate labeling, which cannot bind SKOV-3 cells, exhibited no effects on cell growth and survival, indicating that the folate-pRNA is required for the pRNA dimer chimera to enter cells. Lastly, we performed both cleavage site overlap RT-PCR and a modified[17] 5′-RACE [rapid amplification of complementary DNA (cDNA) ends] PCR, and verified the presence of the specific cleavage product (**Supplementary Figure S6**) indicative of pRNA/siRNA-mediated cleavage of *MT-2A* and *survivin* mRNA.

DISCUSSION

The 117-nt RNA nanoparticle[30] derived from the phi29 DNA-packaging RNA is ideally suited for delivery of siRNA directed toward multiple gene targets.[27,28] It has the potential of being safe, noninfectious/nonpathogenic and resistant to degradation. We investigated the utility of the pRNA nanoparticle as a siMT-IIA fusion chimera to inhibit expression of *MT-IIA*, and induce decreased cell proliferation of pRNA/si(MT2A) chimera–transfected cells. We found that the pRNA/siRNA was processed by dicer (**Figure 1**, **Supplementary Figure S7**), localized to GW182 containing speckles, and inhibited the expression of the target

gene. Moreover, transfection of both pRNA/si(MT2A) and pRNA/si(Surv) individually and together, decreased cell proliferation. We found similar results in breast and prostate cancer cells (data not shown). Thus, in addition to *survivin,*[22] targeting *MT-IIA* gene expression could be a second molecule in the arsenal for treating ovarian cancers, and this pRNA nanoparticle, is excellent for delivery of highly potent siRNA.

For the pRNA/siRNA to efficiently function in RNAi, it has to be correctly processed by dicer,[42,43] and delivered to the GW-rich bodies. We have shown that both events occur and that the pRNA/siRNA chimera is highly efficient in triggering RNAi. It has recently been described[16,20] that RNAi by chemically synthesized d-siRNA duplexes in the 25–30 base length range are more potent than 21-mer siRNAs in the same location. The observed increased potency obtained using longer d-siRNAs in triggering RNAi is thought to result from providing dicer with a substrate instead of a product, which improves the rate or efficiency of entry of the d-siRNA into RISC as facilitated by dicer.[44] Alternatively, this could be due to the pRNA/siRNA-processed RISC-siRNA functioning as a multiple-turnover enzyme that recognizes and cleaves its target multiple times resulting in a more potent, longer-lasting effect. It should be noted that although 33 nmol/l siMT-IIA had similar gene silencing efficiency as 2 nmol/l pRNA/si(MT2A), the siRNA was less potent than the corresponding pRNA/siRNA at decreasing cell survival. Because negligible amounts of IFN-α and IFN-β were detected, this was not a toxicity issue. We reasoned that this could be a question of relative pRNA stability within cells, because the RNA expression studies and cell proliferation studies were performed at different time points. The siRNA might be more prone to degradation than pRNA/siRNA, and thus less effective in the long term. Alternatively, the GW/P bodies are believed to be sites of mRNA degradation as well as translational repression.[45] A working model for how RISC interacts with cytoplasmic mRNAs has been proposed[45] where siRNA-RISC first interacts with its target mRNA. If this interaction is stable, RISC remains bound leading to translational repression and the accumulation of the mRNA/RISC in GW/P-bodies, although the molecular details of that effect remain unclear. Moreover, if RISC contains a cleavage-competent Ago protein, the mRNA is cleaved before, during, or after accumulation of the mRNA:RISC in GW/P-bodies. The stage at which endonuclease cleavage occurs would simply be a function of the relative rates of cleavage versus translation repression and GW/P-body accumulation. We found that the siRNA of pRNA/siRNA was more stable within cells, and present within the GW/P-bodies 6 days post-transfection (**Supplementary Figure S2**). Because *MT* is an extremely small protein (~7 kDa) and *MT-IIA* isoform antibodies cross-react with *MT-I*, we could not analyze *MT-IIA* by western blot. However, we immunostained pRNA/si(MT2A)-transfected cells for MT expression and found lower levels of staining intensity in pRNA/si(MT2A)-transfected cells compared to control cells (**Supplementary Figure S3**). Moreover, we used cleavage site overlap RT-PCR to confirm mRNA cleavage of *MT-2A* and *survivin* in pRNA/si(MT2A)- and pRNA/si(Surv)-transfected cells (**Supplementary Figure S4**).

Relatively subtle perturbations of anti-apoptotic protein expression, stability or binding to associated molecules can irreversibly impair cell viability. We observed that although the expression of *survivin* mRNA decreased by 20% on transfection of pRNA/si(Surv) in SKOV-3 and OVCA 433 cells, its effects on cell proliferation was >20%, depending on cell type. This could be due to the fact that *survivin* expression in SKOV-3 and OVCA 433 cells is three- to sixfold lower than that present in OVCA 432 cells. Once survivin expression fell below a threshold level, cell death was triggered. Hence, even a 20–30% decrease in *survivin* in SKOV-3 and OVCA 433 cells was sufficient to trigger cell death.

The ability of pRNA chimeras to form dimers makes them extremely useful for targeted delivery of siRNA into cancer cells. We showed that the pRNA/siRNA-folate-pRNA dimer can deliver siRNA to folate receptor-α expressing ovarian carcinoma cells.[21] However, only 15% of the folate-pRNA dimer bound to cells. Previous studies have indicated that pRNA forms dimers with high efficiency which are very stable in solutions.[46–48] The low binding efficiency to cells may reflect the degradation of pRNA in serum. To compensate for the low folate-pRNA dimer cell-binding activity, we have performed two rounds of treatment with folate-pRNA-pRNA/siRNA dimers, and observed a significant decrease in cell survival in the presence of *MT-IIA* and *survivin* targeting pRNA/siRNA, indicating the high potential of this delivery system. We are working on making the pRNA resistant to degradation, a key step essential for transition to preclinical animal trials. As a consequence of our findings, we can envision future studies aimed at cancer cell–specific, folate-mediated uptake of siRNA targeting *survivin* and *MT-IIA* as a pRNA trimer. This strategy has the potential for targeting a single cell with multiple molecules, making pRNA nanoparticle-mediated delivery ideally suited to overcome the extraordinary heterogeneity of human cancer.

In summary, we have shown that: (i) pRNA/siRNA chimera can be efficiently processed by dicer and are localized within the GW/P-bodies, (ii) pRNA/si(MT2A) is more efficient than siRNA alone in silencing *MT-IIA* expression, (iii) pRNA/si(MT2A) and pRNA/si(Surv) can be used to specifically silence *MT-IIA* and *survivin* mRNA expression, respectively, leading to decreased cell proliferation, (iv) folate-mediated uptake of pRNA/si(MT2A) and pRNA/si(Surv) can inhibit cell growth/survival, and (v) the combination of pRNA/siRNA targeted toward *survivin* and *MT-IIA* leads to more potent effects on cell proliferation. Thus, the pRNA/si(MT2A) chimera provides another robust subunit for construction of pRNA-based multivalent therapeutic vehicle against cancer cells.

MATERIALS AND METHODS

Cell culture. Ovarian cancer cell line SKOV-3, nasopharyngeal carcinoma KB cells (American Type Culture Collection, Manassas, VA), and the primary human Ovarian Cancer (OVCA 432 and OVCA 433) and the ovarian surface epithelial (HOSE 642) cell lines have been described previously[31,32] and are routinely maintained in RPMI 1640 medium and supplemented with 10% fetal bovine serum. Cultures were incubated at 37 °C in a humidified 5% CO_2 atmosphere; 7,000 cells were seeded into each well of a 96-well culture plate (Nunc, Rochester, NY) for *in vitro* experiments.

Nomenclature, construction, and synthesis of RNA. The nomenclature of pRNA and the resulting chimeric pRNA subunits for the construction of siRNA nanoparticles have been reported.[23] Briefly, upper-case and lower-case letters are used to represent the right and left hand loops of the pRNA, respectively. Matched letters indicate complementarity, whereas different letters indicate no complementary loops. For example, Ab′pRNA contains right hand loop A (5′ $G_{45}G_{46}A_{47}C_{48}$) and left hand loop b′ (3′ $U_{85}G_{84}C_{83}G_{82}$),

which can pair with the left hand loop a′ (3′ $C_{85}C_{84}U_{83}G_{82}$) and right hand loop B (5′ $A_{45}C_{46}G_{47}C_{48}$), respectively, of Ba′pRNA (**Figure 1a**).

The synthesis of RNA has been described previously.[29] Approximately 10 mmol/l of magnesium chloride was included in all buffers to maintain the intermolecular interaction and folding of pRNA.[21,22] The DNA primers for chimera pRNA/siRNA transcription were ordered from Sigma, St Louis, MO. The DNA products containing the T7 polymerase class II promoter as previously described,[21,22] were used as substrates for direct *in vitro* transcription using RiboMAX T7 kit (Promega, Madison, WI). pRNA/si(Surv) represents a pRNA chimera that harbors a siRNA targeting *survivin*;[21] pRNA/si(MT2-1) and pRNA/si(MT2-2) represent pRNA chimeras that harbor siRNA targeting *MT-IIA* sequences "GCAAAGGGGCGTCGG ACAA" and "GCGTCGGACAAGTGCAGCT," respectively. The pRNA/si(CONT2) chimera contains a random sequence, same as that in siCONT2 (Dharmacon, Lafayette, CO) which has been tested by the manufacturer not to downregulate the expression of any mRNA. The transcribed pRNA/siRNA were resolved on a 6% PAGE/urea gel for size and on a 8% Tris–borate–magnesium chloride PAGE for dimerization studies as previously described.[49] Fluorescent pRNA/si(CONT2) chimera was generated using the Cy3 Silencer siRNA labeling kit (Applied Biosystems/Ambion, Austin, TX) in accordance with the manufacturer's instructions.

siRNA- and pRNA/siRNA-mediated downregulation of* survivin *and the* MT-IIA *isoform. All siRNAs were ordered from IDT (Coralville, IA). siCONT2 (UAAGGCUAUGAAGAGAUAC) was used as the negative control (Dharmacon, Lafayette, CO) and siMT2-1 and siMT2-2 (GCAAAGG GGCGTCGGACAA and GCGUCGGACAAGUGCAGCU, respectively) were used to target *MT-IIA*. Ovarian cancer cells were transfected with reconstituted siRNA silencing duplex diluted in opti-MEM I Reduced Serum Medium (Invitrogen). Intracellular delivery of the siRNA or pRNA/siRNA was facilitated by use of lipofectamine 2000 transfection reagent (Invitrogen) according to the manufacturer's protocol. Transfected cells were first incubated for 5 hours prior to fresh medium replacement and maintained for another 72 hours before further analysis.

Cell proliferation analyses. Cells were transfected in triplicate with the Ba′pRNA/siRNA using lipofectamine 2000 (Invitrogen). Alternatively, for the folate-pRNA-pRNA/siRNA dimer studies, cells in 96-well plates were treated with 200 and 400 nmol/l folate-pRNA dimer complexes in HEPES-buffered saline (HBS) containing 10 mmol/l magnesium chloride for 30 minutes. The HBS was removed and replaced with culture media. Treatments were performed twice, on day 1 and 3. Cell proliferation was evaluated using the tetrazolium salt containing CellTiter 96 AQ_{ueous} One Solution Cell Proliferation assay (Promega). Three days post-transfection and 4 days after the first treatment, the culture media were removed and replaced with 60 µl CellTiter 96 AQ_{ueous} One Solution reagent mix in each well according to the manufacturer's protocol. Cells were incubated at 37 °C for 60 minutes. Absorbance was measured at 490 nm. Experiments were performed at least twice, in triplicate, and the percentage of surviving cells for each well was calculated as follows:

$$\%\ \text{proliferation} = \frac{\text{optical density (OD) of test sample}}{\text{OD of control sample}} \times 100\%.$$

Results are presented as average ± SD of triplicate experiments.

Real-time RT-PCR analysis. Total RNA was isolated using TRIzol (Invitrogen) and reverse transcribed using the SuperScript III First-Strand Synthesis System (Invitrogen). Single-stranded cDNA then served as template for real-time PCR analysis performed using the 7900HT Real-Time PCR System (Applied Biosystems, Foster City, CA), employing the SYBR Green reagent (Invitrogen). The primers used for the detection of the *MT-IIA* isoform was adapted from Mididoddi *et al.*[50] *GAPDH* and *survivin* were detected by the following pairs of primers: 5′-GAAGGTGAAGGTCGGAGT CA-3′ (forward) and 5′-GACAAGCTTCCCGTTCTCAG-3′ (reverse); and 5′-GACCCGTTGGCAGAGGTG-3′ (forward) and 5′-TTCTCAGTGGGG CAGTGGAT-3′ (reverse), respectively. The cDNA sample was subjected to 40 PCR cycles of denaturation at 94 °C for 15 seconds, and annealing and elongation of primer at 60 °C for 45 seconds after an initial activation of Taq polymerase at 95 °C for 15 minutes. To confirm the specificity of the amplification process, a melting curve analysis was performed, together with gel electrophoresis of the resulting PCR products. Relative quantification was calculated using the C_t method, where ΔC_t is equal to the difference between the C_t values of the target gene and the housekeeping *GAPDH* gene.

Statistical analysis. Each experiment was performed in triplicate, the mean ± SEM calculated for variables in each experimental group and analyzed by the Student's *t*-test (two-tailed). *P* values of <0.05 were considered significant.

Chimeric pRNA/siRNA processing by dicer. Chimeric pRNA/siRNAs were incubated with purified recombinant RNA-specific endonuclease (dicer; Genlantis, San Diego, CA) for 2 hours at 37 °C. The digested fragments were resolved on a 20% PAGE/urea gel.

Immunofluorescent microscopy. For immunofluorescence imaging, cells were transfected with Cy3-labeled Ba′pRNA/si(CONT2). Twenty-four hours post-transfection, cells were fixed with 4% formalin/5% acetic acid for half an hour, followed by 0.5% Triton X-100/phosphate-buffered saline (PBS) treatment (10 minutes) to permeabilize the cells. Slides were blocked with normal chicken serum, stained with mouse monoclonal anti-GW182 antibody (Clone 4B6; Abcam, Cambridge, MA) diluted 1:100 in PBS (1 hour). Alexa Fluor 488–coupled chicken anti-mouse secondary antibody (Invitrogen) was used at a dilution of 1:500. Cells were mounted using ProLong Gold Antifade Reagent with 4′,6-diamidino-2-phenylindole (Invitrogen).

Design of folate-pRNA, flow cytometric analysis, and confocal microscopy. 5′-End folate-labeled DNA oligonucleotide was obtained by 1-ethyl-3-(3-dimethylaminopropyl) carbodiimide– (Thermo Fisher Scientific, Rockford, IL) mediated $–NH_2$ group and folate-chemical reaction. The DNA was annealed with the pRNA (22/98 *Sph*I Ab′pRNA) to generate folate-pRNA. The annealed products (folate-pRNA, NH_2-pRNA) were purified from 8% PAGE/urea denaturing gel.

The cell-binding studies were performed on KB cells which were maintained in folate-free RPMI 1640 medium overnight. The complementary pRNA/siRNA was stained with Cy3 fluorophores by Silencer siRNA labeling kit (Applied Biosystems) as per manufacturer's instructions prior to cell-binding studies. Approximately 700 nmol/l folate-pRNA and control NH_2-pRNA were each incubated with the complementary Cy3-pRNA/siRNA to form dimers. The dimers were then assayed for binding by incubation with 2×10^5 KB cells at 37 °C for 1 hour. After PBS wash, the cells were resuspended in PBS buffer. In competition experiments, the cells were incubated with a 100-fold molar excess of free folate in presence of the pRNA dimers. Fluorescent Microscope (Olympus, Center Valley, PA) and Flow Cytometry (Beckman Coulter, Brea, CA) were used to observe the cell-binding efficacy of folate-pRNA complex.

For confocal microscopy, cells were grown on glass coverslips in folate-free medium overnight. Approximately 700 nmol/l folate-pRNA and control NH_2-pRNA were each incubated with the complementary Cy3-pRNA/siRNA to form dimers. The dimers were then assayed for binding and cell entry by incubation with cells at 37 °C for 2–3 hours. After PBS wash, the cells were fixed by 4% paraformaldehyde and stained by Alexa Fluor 488 phalloidin (Invitrogen) for cytoskeleton and TO-PRO-3 iodide (642/661) (Invitrogen) for nucleus as per manufacturer's instructions. Confocal images were taken by the Zeiss LSM 510 laser scanning confocal microscope.

SUPPLEMENTARY MATERIAL

Figure S1. pRNA/siRNA do not induce high levels of interferon-α and β expression.
Figure S2. Cy3-Ba'pRNA/si(CONT2) is localized within discrete speckles at 6 days post-transfection.
Figure S3. Immunofluorescence staining for MT expression.
Figure S4. Cleavage site overlap RT-PCR to demonstrate decreased levels of *MT-2A* and *survivin* products in pRNA/si(MT2A) and pRNA/si(Surv) transfected cells.
Figure S5. Binding and entry of folate-labeled folate-pRNA-Cy3-pRNA/siRNA dimer particle.
Figure S6. Silencing of targeted *MT-IIA* or s*urvivin.*
Figure S7. Dicer processing of pRNA/siRNA.

ACKNOWLEDGMENTS

This work was supported in part by the National Institutes of Health grants PN2 EY 018230, CA112570, ES006096, and EB003730, and by the Department of Defense grant W81XWH-10-1-0367 (PC094619). We are grateful to Ricky Yuet-Kin Leung and Amy Fullenkamp (University of Cincinnati) for helpful discussion and reading of the manuscript. P.G. is the co-founder of Kylin Therapeutics, Inc.

REFERENCES

1. Altieri, DC (2008). Survivin, cancer networks and pathway-directed drug discovery. *Nat Rev Cancer* **8**: 61–70.
2. Ferrandina, G, Legge, F, Martinelli, E, Ranelletti, FO, Zannoni, GF, Lauriola, L *et al.* (2005). Survivin expression in ovarian cancer and its correlation with clinico-pathological, surgical and apoptosis-related parameters. *Br J Cancer* **92**: 271–277.
3. Liguang, Z, Peishu, L, Hongluan, M, Hong, J, Rong, W, Wachtel, MS *et al.* (2007). Survivin expression in ovarian cancer. *Exp Oncol* **29**: 121–125.
4. Sui, L, Dong, Y, Ohno, M, Watanabe, Y, Sugimoto, K and Tokuda, M (2002). Survivin expression and its correlation with cell proliferation and prognosis in epithelial ovarian tumors. *Int J Oncol* **21**: 315–320.
5. Pennati, M, Folini, M and Zaffaroni, N (2008). Targeting survivin in cancer therapy. *Expert Opin Ther Targets* **12**: 463–476.
6. Hussain, S, Slikker, W Jr and Ali, SF (1996). Role of metallothionein and other antioxidants in scavenging superoxide radicals and their possible role in neuroprotection. *Neurochem Int* **29**: 145–152.
7. Jin, R, Chow, VT, Tan, PH, Dheen, ST, Duan, W and Bay, BH (2002). Metallothionein 2A expression is associated with cell proliferation in breast cancer. *Carcinogenesis* **23**: 81–86.
8. Zagorianakou, N, Stefanou, D, Makrydimas, G, Zagorianakou, P, Briasoulis, E, Karavasilis, V *et al.* (2006). Clinicopathological study of metallothionein immunohistochemical expression, in benign, borderline and malignant ovarian epithelial tumors. *Histol Histopathol* **21**: 341–347.
9. McCluggage, WG, Strand, K and Abdulkadir, A (2002). Immunohistochemical localization of metallothionein in benign and malignant epithelial ovarian tumors. *Int J Gynecol Cancer* **12**: 62–65.
10. Klaassen, CD and Liu, J (1998). Metallothionein transgenic and knock-out mouse models in the study of cadmium toxicity. *J Toxicol Sci* **23** (suppl. 2): 97–102.
11. Tekur, S and Ho, SM (2002). Ribozyme-mediated downregulation of human metallothionein II(a) induces apoptosis in human prostate and ovarian cancer cell lines. *Mol Carcinog* **33**: 44–55.
12. Abdel-Mageed, A and Agrawal, KC (1997). Antisense down-regulation of metallothionein induces growth arrest and apoptosis in human breast carcinoma cells. *Cancer Gene Ther* **4**: 199–207.
13. Lim, D, Jocelyn, KM, Yip, GW and Bay, BH (2009). Silencing the Metallothionein-2A gene inhibits cell cycle progression from G1- to S-phase involving ATM and cdc25A signaling in breast cancer cells. *Cancer Lett* **276**: 109–117.
14. Kim, DH, Behlke, MA, Rose, SD, Chang, MS, Choi, S and Rossi, JJ (2005). Synthetic dsRNA Dicer substrates enhance RNAi potency and efficacy. *Nat Biotechnol* **23**: 222–226.
15. Scherer, LJ and Rossi, JJ (2003). Approaches for the sequence-specific knockdown of mRNA. *Nat Biotechnol* **21**: 1457–1465.
16. Rose, SD, Kim, DH, Amarzguioui, M, Heidel, JD, Collingwood, MA, Davis, ME *et al.* (2005). Functional polarity is introduced by Dicer processing of short substrate RNAs. *Nucleic Acids Res* **33**: 4140–4156.
17. McNamara, JO 2nd, Andrechek, ER, Wang, Y, Viles, KD, Rempel, RE, Gilboa, E *et al.* (2006). Cell type-specific delivery of siRNAs with aptamer-siRNA chimeras. *Nat Biotechnol* **24**: 1005–1015.
18. Zhou, J, Li, H, Li, S, Zaia, J and Rossi, JJ (2008). Novel dual inhibitory function aptamer-siRNA delivery system for HIV-1 therapy. *Mol Ther* **16**: 1481–1489.
19. Merkel, OM, Beyerle, A, Librizzi, D, Pfestroff, A, Behr, TM, Sproat, B *et al.* (2009). Nonviral siRNA delivery to the lung: investigation of PEG-PEI polyplexes and their *in vivo* performance. *Mol Pharm* **6**: 1246–1260.
20. Amarzguioui, M, Rossi, JJ and Kim, D (2005). Approaches for chemically synthesized siRNA and vector-mediated RNAi. *FEBS Lett* **579**: 5974–5981.
21. Guo, S, Huang, F and Guo, P (2006). Construction of folate-conjugated pRNA of bacteriophage phi29 DNA packaging motor for delivery of chimeric siRNA to nasopharyngeal carcinoma cells. *Gene Ther* **13**: 814–820.
22. Guo, S, Tschammer, N, Mohammed, S and Guo, P (2005). Specific delivery of therapeutic RNAs to cancer cells via the dimerization mechanism of phi29 motor pRNA. *Hum Gene Ther* **16**: 1097–1109.
23. Khaled, A, Guo, S, Li, F and Guo, P (2005). Controllable self-assembly of nanoparticles for specific delivery of multiple therapeutic molecules to cancer cells using RNA nanotechnology. *Nano Lett* **5**: 1797–1808.
24. Shu D, Moll WD, Deng Z, Mao C and Guo P (2004). Bottom-up assembly of RNA arrays and superstructures as potential parts in nanotechnology. *Nano Lett* **4**: 1717–1723.
25. Guo, P, Zhang, C, Chen, C, Garver, K and Trottier, M (1998). Inter-RNA interaction of phage phi29 pRNA to form a hexameric complex for viral DNA transportation. *Mol Cell* **2**: 149–155.
26. Guo, PX, Erickson, S and Anderson, D (1987). A small viral RNA is required for *in vitro* packaging of bacteriophage phi 29 DNA. *Science* **236**: 690–694.
27. Chen, C, Sheng, S, Shao, Z and Guo, P (2000). A dimer as a building block in assembling RNA. A hexamer that gears bacterial virus phi29 DNA-translocating machinery. *J Biol Chem* **275**: 17510–17516.
28. Shu, D, Huang, LP, Hoeprich, S and Guo, P (2003). Construction of phi29 DNA-packaging RNA monomers, dimers, and trimers with variable sizes and shapes as potential parts for nanodevices. *J Nanosci Nanotechnol* **3**: 295–302.
29. Zhang, C, Lee, CS and Guo, P (1994). The proximate 5′ and 3′ ends of the 120-base viral RNA (pRNA) are crucial for the packaging of bacteriophage phi 29 DNA. *Virology* **201**: 77–85.
30. Trottier, M, Mat-Arip, Y, Zhang, C, Chen, C, Sheng, S, Shao, Z *et al.* (2000). Probing the structure of monomers and dimers of the bacterial virus phi29 hexamer RNA complex by chemical modification. *RNA* **6**: 1257–1266.
31. Syed, V, Ulinski, G, Mok, SC and Ho, SM (2002). Reproductive hormone-induced, STAT3-mediated interleukin 6 action in normal and malignant human ovarian surface epithelial cells. *J Natl Cancer Inst* **94**: 617–629.
32. Lau, KM, Mok, SC and Ho, SM (1999). Expression of human estrogen receptor-alpha and -beta, progesterone receptor, and androgen receptor mRNA in normal and malignant ovarian epithelial cells. *Proc Natl Acad Sci USA* **96**: 5722–5727.
33. Lee, KF, Lau, KM and Ho, SM (1999). Generation and characterization of hammerhead ribozymes targeting rodent metallothionein-I and -II ribonucleic acid. *Toxicol Appl Pharmacol* **161**: 294–301.
34. Kim, DH, Longo, M, Han, Y, Lundberg, P, Cantin, E and Rossi, JJ (2004). Interferon induction by siRNAs and ssRNAs synthesized by phage polymerase. *Nat Biotechnol* **22**: 321–325.
35. Jakymiw, A, Lian, S, Eystathioy, T, Li, S, Satoh, M, Hamel, JC *et al.* (2005). Disruption of GW bodies impairs mammalian RNA interference. *Nat Cell Biol* **7**: 1267–1274.
36. Liu, J, Rivas, FV, Wohlschlegel, J, Yates, JR 3rd, Parker, R and Hannon, GJ (2005). A role for the P-body component GW182 in microRNA function. *Nat Cell Biol* **7**: 1261–1266.
37. Gibbings, DJ, Ciaudo, C, Erhardt, M and Voinnet, O (2009). Multivesicular bodies associate with components of miRNA effector complexes and modulate miRNA activity. *Nat Cell Biol* **11**: 1143–1149.
38. Jagannath, A and Wood, MJ (2009). Localization of double-stranded small interfering RNA to cytoplasmic processing bodies is Ago2 dependent and results in up-regulation of GW182 and Argonaute-2. *Mol Biol Cell* **20**: 521–529.
39. Li, S, Lian, SL, Moser, JJ, Fritzler, ML, Fritzler, MJ, Satoh, M *et al.* (2008). Identification of GW182 and its novel isoform TNGW1 as translational repressors in Ago2-mediated silencing. *J Cell Sci* **121**: 4134–4144.
40. Lian, S, Fritzler, MJ, Katz, J, Hamazaki, T, Terada, N, Satoh, M *et al.* (2007). Small interfering RNA-mediated silencing induces target-dependent assembly of GW/P bodies. *Mol Biol Cell* **18**: 3375–3387.
41. Parker, N, Turk, MJ, Westrick, E, Lewis, JD, Low, PS and Leamon, CP (2005). Folate receptor expression in carcinomas and normal tissues determined by a quantitative radioligand binding assay. *Anal Biochem* **338**: 284–293.
42. Chu, CY and Rana, TM (2008). Potent RNAi by short RNA triggers. *RNA* **14**: 1714–1719.
43. Pham, JW, Pellino, JL, Lee, YS, Carthew, RW and Sontheimer, EJ (2004). A Dicer-2-dependent 80s complex cleaves targeted mRNAs during RNAi in Drosophila. *Cell* **117**: 83–94.
44. Amarzguioui, M, Lundberg, P, Cantin, E, Hagstrom, J, Behlke, MA and Rossi, JJ (2006). Rational design and *in vitro* and *in vivo* delivery of Dicer substrate siRNA. *Nat Protoc* **1**: 508–517.
45. Valencia-Sanchez, MA, Liu, J, Hannon, GJ and Parker, R (2006). Control of translation and mRNA degradation by miRNAs and siRNAs. *Genes Dev* **20**: 515–524.
46. Robinson, MA, Wood, JP, Capaldi, SA, Baron, AJ, Gell, C, Smith, DA *et al.* (2006). Affinity of molecular interactions in the bacteriophage phi29 DNA packaging motor. *Nucleic Acids Res* **34**: 2698–2709.
47. Fang, Y, Cai, Q and Qin, PZ (2005). The procapsid binding domain of phi29 packaging RNA has a modular architecture and requires 2′-hydroxyl groups in packaging RNA interaction. *Biochemistry* **44**: 9348–9358.
48. Fang, Y, Shu, D, Xiao, F, Guo, P and Qin, PZ (2008). Modular assembly of chimeric phi29 packaging RNAs that support DNA packaging. *Biochem Biophys Res Commun* **372**: 589–594.
49. Zhang, C, Tellinghuisen, T and Guo, P (1995). Confirmation of the helical structure of the 5′/3′ termini of the essential DNA packaging pRNA of phage phi 29. *RNA* **1**: 1041–1050.
50. Mididoddi, S, McGuirt, JP, Sens, MA, Todd, JH and Sens, DA (1996). Isoform-specific expression of metallothionein mRNA in the developing and adult human kidney. *Toxicol Lett* **85**: 17–27.